

Supplementary Information

Lead-free, air-stable hybrid organic-inorganic perovskite resistive switching memory with ultrafast switching and multilevel data storage

Bohee Hwang¹ and Jang-Sik Lee^{1, 2*}

¹Department of Materials Science and Engineering, Pohang University of Science and Technology (POSTECH), Pohang 37673, Korea

²Department of Materials Science & Engineering, The University of Texas at Dallas, Richardson 75080, TX, USA

*Corresponding Author. E-mail: jangsik@postech.ac.kr

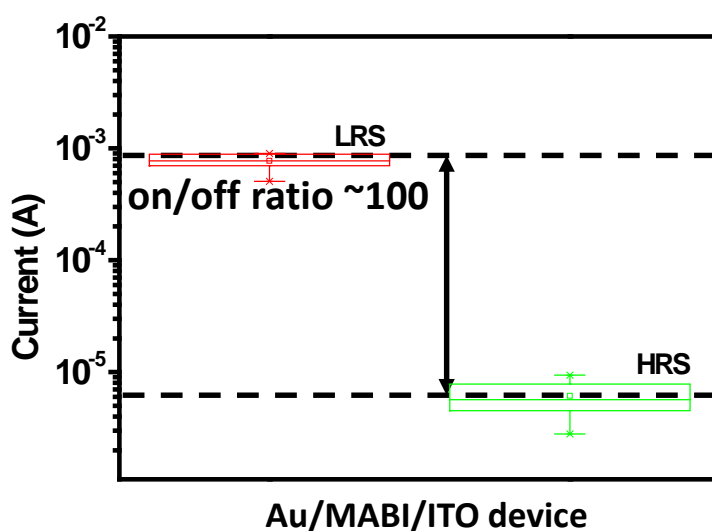


Figure S1. The statistical distribution of LRS and HRS currents in MABI device.

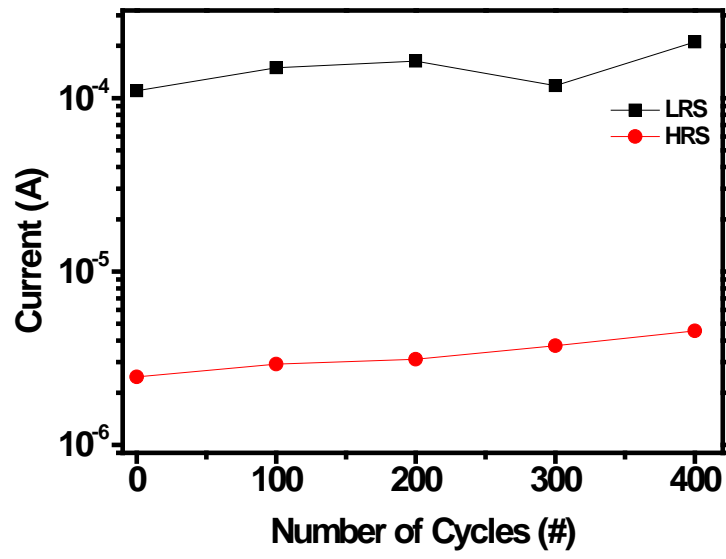


Figure S2. The endurance of memory device based on MABI which is measured using a pulse width of 100 ns. (V_{set} : 3 V, V_{reset} : -3 V, read voltage: 0.2 V)

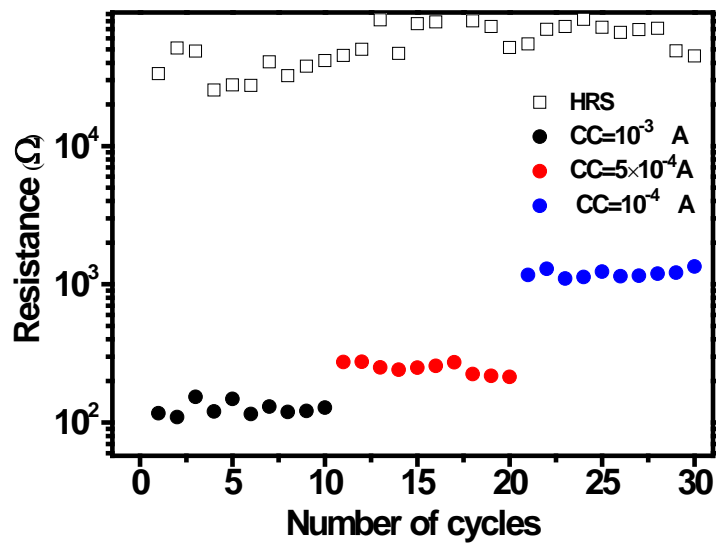


Figure S3. The ac endurance with different compliance of 1 mA, 500 μ A, and 100 μ A.

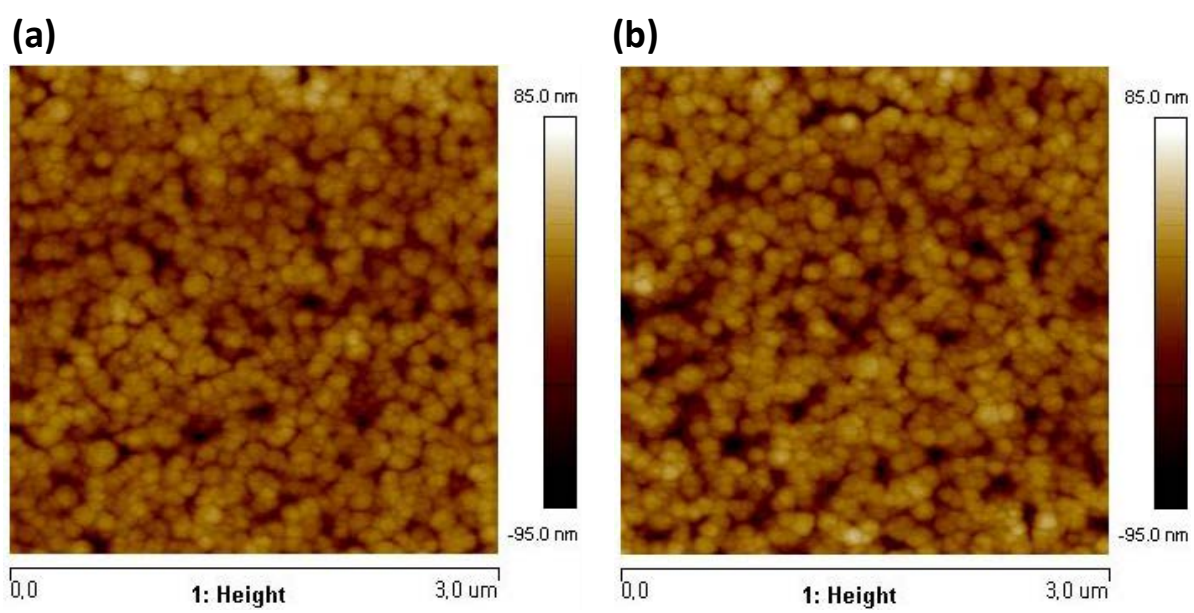


Figure S4. AFM images of (a) the pristine MABI film and (b) MABI film stored in air for 5 months. The scan size of the image was $3\ \mu\text{m} \times 3\ \mu\text{m}$.

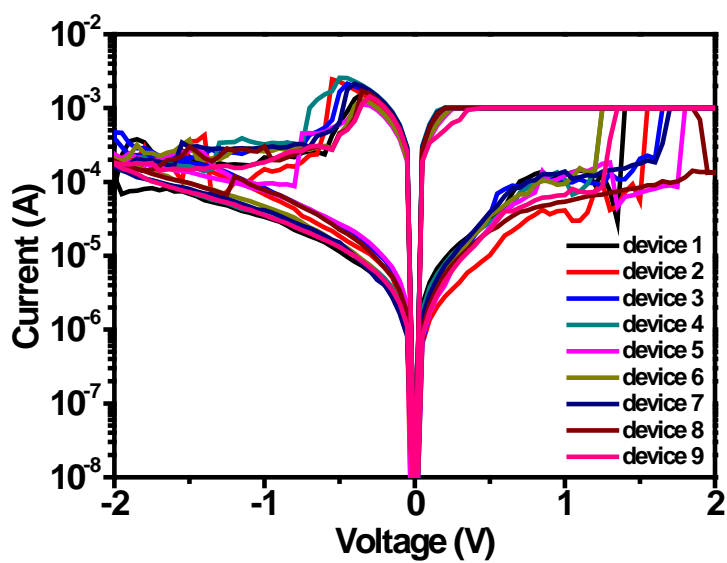


Figure S5. I-V characteristics of Au/MABI/ITO device measured after 5 months of fabrication.

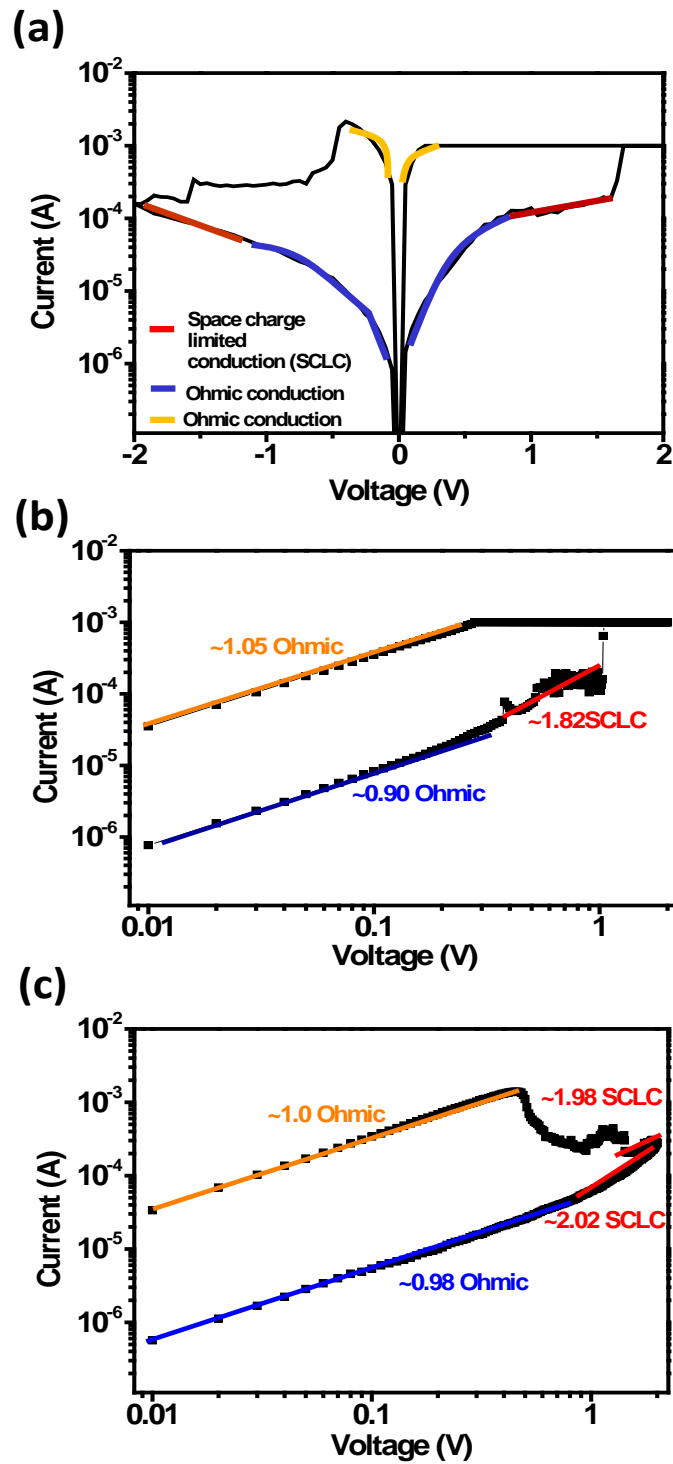


Figure S6. Experimental and fitted *I-V* curves of MABI-based resistive switching memory device. (a) Experimental and fitted semi logarithmic *I-V* curves. (b) Double-logarithmic plots for Au/MABI/ITO device in positive sweep mode and (c) negative sweep mode with the space-charge limited model.

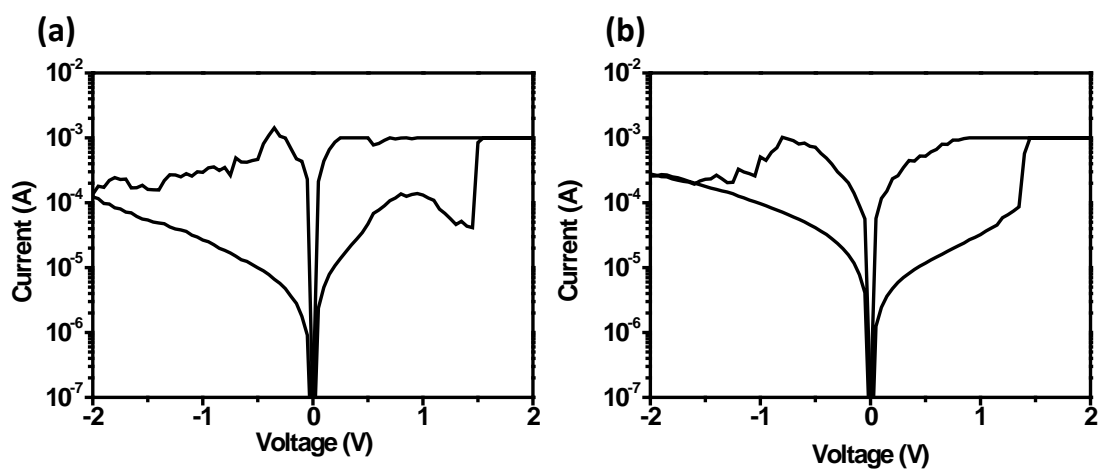


Figure S7. I-V curves of MABI-based memory device with different electrode material. (a) Ag/MABI/ITO/glass and (b) Al/MABI/ITO/glass.

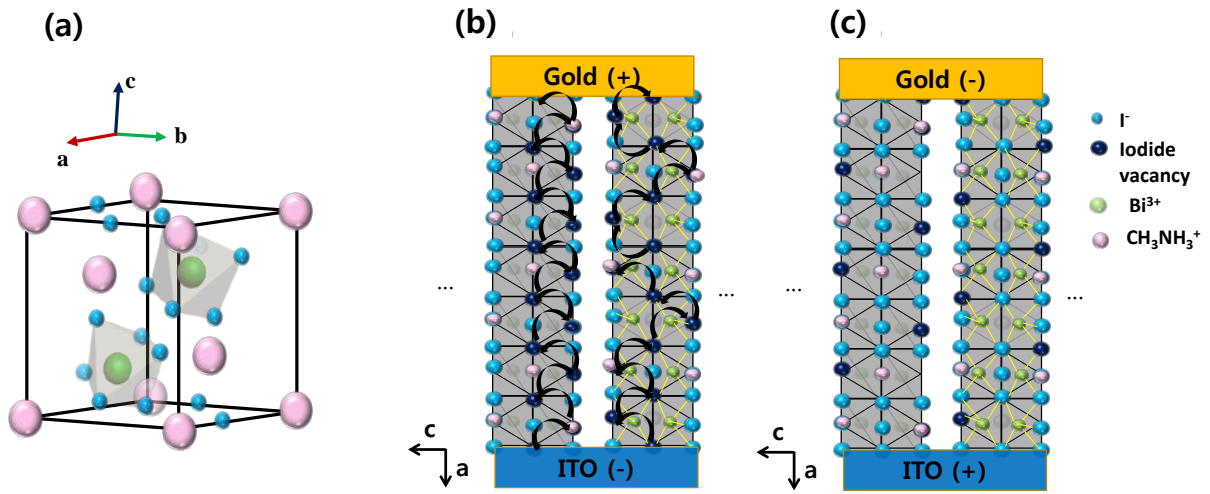


Figure S8. Proposed resistive switching mechanism of MABI-based ReRAM devices. (a) The unit cell of MABI. (b) (010) view of the MABI lattice. Iodide vacancy connected with top and bottom electrodes under positive bias to top electrode. (c) Rupture of filament under negative bias to top electrode.